DMD Fast Forward. Published on December 17, 2007 as doi:10.1124/dmd.107.019703
This article has not been copyedited and formatted. The final version may differ from this version.

DMD # 19703

Regulation of Aryl Hydrocarbon Receptor Expression and Function by Glucocorticoids in Mouse Hepatoma Cells

Kirsten A. Bielefeld, Chunja Lee, and David S. Riddick

Department of Pharmacology & Toxicology, Medical Sciences Building,

University of Toronto, Toronto, Ontario, Canada

Running Title: Glucocorticoid regulation of aryl hydrocarbon receptor

Corresponding Author: David S. Riddick, Department of Pharmacology & Toxicology, Medical Sciences Building, University of Toronto, Toronto, Ontario, Canada M5S 1A8.

Tel: (416) 978-0813; Fax: (416) 978-6395.

E-mail: david.riddick@utoronto.ca

Number of Text Pages: 34

Number of Tables: 0

Number of Figures: 8

Number of References: 40

Words in Abstract: 214

Words in Introduction: 686

Words in Discussion: 1498

ABBREVIATIONS: ADX, adrenalectomy or adrenalectomized; AHR, aryl hydrocarbon receptor; ARNT, aryl hydrocarbon receptor nuclear translocator; CORT, corticosterone; DEX, dexamethasone; DMSO, dimethylsulfoxide; DRE, dioxin-responsive element; EROD, 7-ethoxyresorufin O-deethylation; GR, glucocorticoid receptor; GRE, glucocorticoid-responsive element; HAH, halogenated aromatic hydrocarbon; HYPX, hypophysectomy or hypophysectomized; MC, 3-methylcholanthrene; PAH, polycyclic aromatic hydrocarbon; P450, cytochrome P450; PXR, pregnane X receptor; RT-PCR, reverse transcriptase-polymerase chain reaction; TAT, tyrosine aminotransferase; TCDD, 2,3,7,8-tetrachlorodibenzo-*p*-dioxin; TCDF, 2,3,7,8-tetrachlorodibenzofuran; TSA, trichostatin A.

ABSTRACT

The aryl hydrocarbon receptor (AHR) is a ligand-activated transcription factor that mediates most biological responses to 2,3,7,8-tetrachlorodibenzo-*p*-dioxin (TCDD) and related aromatic hydrocarbons. Although the AHR's role in control of drug metabolism and endocrine disruption is partly understood, we know little about the regulation of the AHR itself by endocrine factors. Our work with hypophysectomized rats suggested that hepatic AHR protein level is positively regulated by pituitary-dependent factors. A current hypothesis is that adrenal glucocorticoids elevate AHR expression and enhance responsiveness to AHR agonists. Dexamethasone (DEX) at concentrations that activate the glucocorticoid receptor (GR) increased AHR mRNA, protein and TCDD-binding by approximately 50% in Hepa-1 mouse hepatoma cells. This response was blocked by the GR antagonist RU486, suggesting GR involvement. This small magnitude increase in AHR levels was functionally significant; pre-treatment of Hepa-1 cells with DEX caused a 75% increase in the maximum induction of an AHR-activated luciferase reporter plasmid by TCDD. A luciferase reporter under control of the proximal 2.5-kb of the mouse *Ahr* 5'-flanking region and promoter was induced approximately 2.5-fold by DEX when co-transfected with a mouse GR expression plasmid. This is the first demonstration that glucocorticoids increase AHR levels in hepatoma cells via a GR-dependent transcriptional mechanism, suggesting a novel aspect of cross-talk between the AHR and the GR.

The aryl hydrocarbon receptor (AHR) is a ligand-activated transcription factor that mediates most biological responses to halogenated aromatic hydrocarbons (HAHs) such as 2,3,7,8-tetrachlorodibenzo-*p*-dioxin (TCDD) and polycyclic aromatic hydrocarbons (PAHs) such as 3-methylcholanthrene (MC). The most fully understood AHR-mediated biological response is the induction of cytochrome P450 (P450) genes belonging to the *CYP1A* subfamily. Binding of ligand to the cytoplasmic AHR complex triggers the translocation of the receptor into the nucleus, dimerization with the AHR nuclear translocator (ARNT), and binding of the AHR•ARNT heterodimer to dioxin-responsive elements (DREs) in regulatory regions of genes subject to transcriptional up-regulation such as *CYP1A1* (Riddick et al., 1994). Although the AHR's role in control of drug metabolism and endocrine disruption is partly understood (Safe, 1995), we know little about the regulation of the AHR itself by endocrine and other factors (Harper et al., 2006).

Our interest in endocrine control of AHR expression and function was stimulated by our observation that hypophysectomy (HYPX) results in a significant loss of hepatic AHR protein and TCDD-binding capacity in male rats without decreasing CYP1A1 induction in response to MC treatment (Timsit et al., 2002). This finding suggested that pituitary hormones and/or pituitary-dependent factors may act as positive regulators of hepatic AHR levels and aromatic hydrocarbon responsiveness. We are interested in identifying the pituitary-dependent factors that modulate hepatic AHR expression and function and determining the molecular mechanisms by which they act.

Our initial focus has been on adrenal glucocorticoids as potential candidates for the pituitary-dependent endocrine factors involved in modulation of AHR levels and activity. Several lines of evidence suggest that glucocorticoids can augment aromatic hydrocarbon responsiveness. Elevated levels of endogenous corticosterone (CORT) induced by stress result in enhanced induction of hepatic CYP1A1-catalyzed 7-ethoxyresorufin O-deethylation (EROD) in response to PAH exposure in rats (Konstandi et al., 2000). The *in vivo* induction of rat hepatic CYP1A1 and/or associated catalytic activities by MC is potentiated by the synthetic glucocorticoid dexamethasone (DEX) (Sherratt et al., 1989) and diminished by adrenalectomy (ADX) (Nebert and Gelboin, 1969). Cell culture studies in PLHC-1 fish hepatocellular carcinoma cells (Celander et al., 1996) and H4IIE rat hepatoma cells (Lai et al., 2004) confirm that glucocorticoids enhance HAH- and/or PAH-dependent CYP1A induction. The ability of glucocorticoids to enhance the induction of CYP1A1 by PAHs is mediated, at least in part, by the presence of functional glucocorticoid-responsive elements (GREs) in the first intron of the rat *CYP1A1* gene (Mathis et al., 1989). The enhancement of CYP1A inducibility by glucocorticoids may also be mediated in part by alterations in AHR protein levels. Treatment of H4IIE rat hepatoma cells with DEX resulted in increased binding of TCDD to the cytosolic AHR (Wiebel and Cikryt, 1990). Treatment of pregnant mice with cortisol yielded offspring with elevated levels of AHR mRNA and protein in craniofacial tissue (Abbott et al., 1994).

However, other lines of evidence do not support this positive influence of glucocorticoids on the AHR system and aromatic hydrocarbon responsiveness. Treatment of rat mammary fibroblasts with DEX resulted in a decrease in AHR protein levels (Brake et al., 1998). ADX in male rats was reported to have no effect on the TCDD-binding capacity of the hepatic AHR as measured by isoelectric focusing (Carlstedt-Duke et al., 1979). Finally, ADX rats are highly sensitive to TCDD-induced lethality and this toxic response can be ameliorated by CORT

treatment (Gorski et al., 1988); however, modulation of lethality by adrenal steroids could occur via events downstream of the AHR . Although there are certainly effects of glucocorticoids on the AHR pathway, these effects appear to be complex and the molecular mechanisms and functional impacts remain poorly understood.

The goals of the present study were to determine whether glucocorticoids modulate AHR expression and function in Hepa-1 mouse hepatoma cells and to explore the molecular mechanisms involved. Hepa-1 cells express abundant levels of AHR protein and are highly responsive to TCDD and MC treatment (Riddick et al., 1994). These cells also possess a functional GR signaling pathway (Cuthill et al., 1987; Prokipcak and Okey, 1988), making them an excellent cell culture model to examine the influences of glucocorticoids on AHR expression and function.

Materials and Methods

Cell culture. The Hepa-1c1c7 mouse hepatoma cell line was obtained from the American Type Culture Collection (Manassas, VA). Cells were grown as monolayer cultures in α-minimum essential medium supplemented with 10% fetal bovine serum (Invitrogen Corporation, Carlsbad, CA) and maintained in an atmosphere of 5% CO_2 and 95% air at 37°C. According to technical data provided by Invitrogen, our culture conditions resulted in cells being exposed to a background level of approximately 0.1 μM cortisol in the medium.

For experiments involving cytosol and RNA isolation, cells were plated in 55 cm^2 dishes and cultured for approximately 66 h to 65-80% confluence. Cells were then exposed to vehicle alone [0.1% dimethylsulfoxide (DMSO)], CORT (0.1, 1, 10 μM), DEX (0.01, 0.1, 1 μM), RU486 (1 μM), or a combination of DEX (0.1 μM) and RU486 (1 μM). Cells were harvested after a treatment period of 24 h. CORT, DEX, and RU486 were purchased from Sigma Chemical Co. (St. Louis, MO).

Analysis of mRNA levels by semiquantitative reverse transcriptase-polymerase chain reaction (RT-PCR). Total RNA was isolated from Hepa-1 cells by the acid guanidinium thiocyanate-phenol-chloroform extraction method (Chomczynski and Sacchi, 1987) using Tri-Reagent (Sigma Chemical Co.). RNA samples were then treated with 20 U DNase I (GE Healthcare Bio-Sciences, Baie d'Urfé, Quebec, Canada) at 37°C for 20 min to remove genomic DNA contamination. RNA yield and purity were assessed by determining the A_{260}/A_{280} ratio (≥1.7 for all samples), and RNA integrity was assessed by comparing the relative intensities of the 28S and 18S rRNA bands as visualized on ethidium bromide-stained agarose gels. For the reverse transcription step, RNA (1 μg) was incubated with oligo $d(T)_{15}$ (2 μg; Roche

Diagnostics, Laval, Quebec, Canada) at 60°C for 5 min. Primer-annealed samples were then incubated in a final volume of 40 µl with Moloney murine leukemia virus-reverse transcriptase (400 U; Invitrogen), RNA Guard (60 U; GE Healthcare Bio-Sciences), a 1 mM concentration of each 2'-deoxynucleoside 5'-triphosphate (Invitrogen), 10 mM dithiothreitol, and 1X RT buffer containing 50 mM Tris/75 mM KCl/3 mM $MgCl_2$. Reactions were allowed to proceed for 60 min at 37°C, followed by incubation at 70°C for 10 min.

PCR primers were synthesized by ACGT Corporation (Toronto, Ontario, Canada) or Integrated DNA Technologies, Inc. (Coralville, IA). The specificity of primers against the mouse genome was confirmed by BLAST search [www.ncbi.nlm.nih.gov/BLAST/] and by Primer-UniGene Selectivity (PUNS) analysis (Boutros and Okey, 2004). PCR primer sequences were as follows: mouse AHR, 5'-GGTGCCTGCTGGATAATTCATCTG-3' (forward primer) and 5'-TCGTCCTTCTTCATCCGTCAGTG-3' (reverse primer) (Giannone et al., 1998); mouse ß-actin, 5'-CTACAAGAGCTGCGTGTGG-3' (forward primer) and 5'-TAGCTCTTCTCCAG GGAGGA-3' (reverse primer) (Giannone et al., 1998); mouse tyrosine aminotransferase (TAT), 5'-GCCAATCCTGGACAGAACAT-3' (forward primer) and 5'-TTCTGAAGGTGCCGCTTAC T-3' (reverse primer) (Sakuma et al., 2004).

All PCR assays began with a hot start phase, typically 3 or 5 min at 94°C or 95°C, and ended with a final extension phase, typically 7 min at 72°C. Each 50-µl PCR sample contained input cDNA derived from 50 or 75 ng RNA, *Taq* polymerase (10 U; Invitrogen), an appropriate concentration of each primer (0.08 or 0.4 µM), a 1.6 mM concentration of each 2'-deoxy-nucleoside 5'-triphosphate, and 1X PCR buffer containing 20 mM Tris/50 mM KCl/3 mM $MgCl_2$. Cycling conditions were as follows: AHR and ß-actin duplex reaction, (95°C for 20 s, 58°C for 20 s, 72°C for 40s) X 19-21 cycles; TAT, (94°C for 30 s, 53°C for 30 s, 72°C for 40s) X 28-35 cycles. Amplified PCR products (AHR, 503 bp; ß-actin, 450 bp; TAT, 230 bp) were

separated on 6% polyacrylamide gels, stained with Vistra Green (GE Healthcare Bio-Sciences), and quantitated by Phosphorimager analysis (Molecular Dynamics, Sunnyvale, CA) using IPLabGel software (Signal Analytics, Vienna, VA). AHR signal intensity was normalized to the internal reference standard, ß-actin, for semiquantitative analysis. TAT mRNA levels were assessed as a qualitative positive control response. PCR conditions (input cDNA, cycle number) were optimized to yield product within the exponential range of amplification.

Immunoblot analysis. Cytosol was isolated from Hepa-1 cells in HEGD buffer (25 mM Hepes, 1.5 mM EDTA, 10% glycerol, 1 mM dithiothreitol, pH 7.4) by differential centrifugation. Protein concentration was determined by the method of Bradford (1976). Cytosolic protein (10 or 50 µg) isolated from Hepa-1 cells was resolved by SDS-polyacrylamide gel electrophoresis and transferred to nitrocellulose (Hybond-ECL, GE Healthcare Bio-Sciences). For detection of AHR protein, a rabbit polyclonal antibody directed against the N-terminal fragment of the AHR encoded by the b-1 allele (amino acid 1-402) (Pollenz et al., 1994) (Biomol Research Laboratories, Plymouth Meeting, PA) was used at a 1:20,000 dilution, followed by a donkey anti-rabbit Ig-horseradish peroxidase conjugate (GE Healthcare Bio-Sciences) at a dilution of 1:10,000. For detection of GR protein, a rabbit polyclonal antibody directed against a human GR peptide (amino acid 346-367) (Affinity BioReagents, Golden, CO) was used at a concentration of 5 µg/ml, followed by a donkey anti-rabbit Ig-horseradish peroxidase conjugate (GE Healthcare Bio-Sciences) at a dilution of 1:5,000. An enhanced chemiluminescence system (ECL, GE Healthcare Bio-Sciences) was used for protein detection, and films were scanned on a HP Scanjet 3970 scanner (Hewlett-Packard Company, Palo Alto, CA) and relative quantitation was performed using IPLabGel software. Immunoblot quantitative analyses were performed

under conditions that yielded a linear relationship between amount of cytosolic protein and immunoreactive signal intensity.

AHR radioligand binding by sucrose density gradient analysis. Hepa-1 cytosol (0.5 ml, ~2 mg protein/ml) was incubated with 10 nM [^{3}H]TCDD (26.2 to 26.7 Ci/mmol at the time of use; Chemsyn Science Laboratories, Lenexa, KS) in the absence or presence of a 100-fold molar excess of nonradioactive 2,3,7,8-tetrachlorodibenzofuran (TCDF; Dr. Stephen Safe, Texas A&M University, College Station, TX) for 75 min at 4°C. TCDD and TCDF were added to cytosol in DMSO in 5-µl volumes. After incubation, unbound radioligand was removed by treating samples with dextran-coated charcoal (1 mg/mg cytosolic protein) and samples were analyzed by sucrose density gradient centrifugation as described previously (Riddick et al., 1994). Gradients were fractionated using an ISCO Model 640 Fractionator (Instrumentation Specialties Co., Lincoln, NE) and radioactivity in each fraction was measured by liquid scintillation spectrometry.

Electrophoretic mobility shift assay. The following complementary synthetic DNA oligonucleotides were synthesized and purified by Integrated DNA Technologies, Inc.: 5'-GAT CTGGCTCTTCTCACGCAACTCCG-3' and 5'-GATCCGGAGTTGCGTGAGAAGAGCCA-3'. The core nucleotides of a well-characterized DRE from the mouse *Cyp1a1* 5'-flanking region are underlined. These oligonucleotides were annealed and radiolabeled with [γ-^{32}P]ATP (~3000 Ci/mmol; GE Healthcare Bio-Sciences) using T4 polynucleotide kinase (GE Healthcare Bio-Sciences). Hepa-1 cytosol (25 µl; ~2.75 mg protein/ml) was incubated with 20 nM nonradioactive TCDD (Wellington Laboratories Inc., Guelph, Ontario, Canada) or the vehicle DMSO for 2 h at room temperature. TCDD was added to cytosol in DMSO in 1-µl volumes.

Binding reactions were performed in a 25-µl reaction volume containing 16.7 µl of transformed cytosol (~46 µg of protein), poly[d(I-C)] (Roche Diagnostics) (212.5 ng), and ^{32}P-labeled DRE probe (~200,000 cpm, ~0.5 ng) for 15 min at room temperature. Binding reactions were performed in HEGD buffer containing 50 mM NaCl. Protein-DNA complexes were analyzed by electrophoresis on nondenaturing 4% polyacrylamide gels and radioactivity was detected and quantitated by Phosphorimager analysis using IPLabGel software. The difference in signal between TCDD- and DMSO-treated samples was used to calculate the amount of TCDD-inducible DRE binding.

Reporter gene constructs. The promoterless pGL3-Basic luciferase plasmid and the pRL-TK *Renilla* luciferase plasmid, used for normalization of transfection efficiency, were obtained from Promega Corporation (Madison, WI). The pGudluc1.1 plasmid containing the luciferase gene driven by the mouse mammary tumor virus promoter under regulation of a 480-bp fragment from the mouse *Cyp1a1* 5'-flank containing four DREs was provided by Dr. Michael Denison (University of California, Davis, CA) (Garrison et al., 1996). The glucocorticoid-inducible luciferase plasmid, pGRE-luc, was provided by Dr. Gordon Kirby (University of Guelph, Guelph, ON) (Gerbal-Chaloin et al., 2002).

A new luciferase plasmid driven by the proximal 5'-flanking region and promoter of the mouse *Ahr* gene, mAHR-pGL3, was generated as follows. C57BL/6 mouse genomic DNA was used as a template for PCR amplification of a fragment of the mouse *Ahr* gene spanning from position -2451 to +150 [relative to +1 denoting the G residue of the major transcription initiation site (Mimura et al., 1994)]. All numbering of nucleotide positions is according to Build 36 of the February 2006 (mm8) mouse genome assembly found on the UCSC Genome Browser website [http://genome.ucsc.edu/cgi-bin/hgGateway]. PCR primers were obtained from Integrated DNA

Technologies, Inc. and had the following sequences: 5'-AACACTCGAGGTAGACTCCTTCCT AACTCAGCACACT-3' (forward primer) and 5'-CACCGCTCGAGGAGTCCGTCCACCAGT TCGTCCT-3' (reverse primer). Each primer contained a *Xho*I restriction site at the 5'-end to facilitate cloning of the PCR product into the *Xho*I site of the promoterless pGL3-Basic plasmid. The identity of the mAHR-pGL3 reporter plasmid was confirmed by restriction analysis and DNA sequencing.

Transient transfection and luciferase assay. For all transfection studies, Hepa-1 cells were seeded in 12-well plates and cultured for approximately 24 h to 50% confluence, followed by the manipulations described below.

To assess induction of pGudluc1.1 activity by TCDD and MC, cells were initially exposed to vehicle (0.1% DMSO) or DEX (0.1 µM) for 24 h. Following a change of medium, cells were co-transfected with pGudluc1.1 (1.4 µg) and pRL-TK (0.1 µg) using Superfect reagent (Qiagen, Valencia, CA). Immediately after transfection, cells were treated with vehicle (0.1% DMSO), TCDD (1 pM to 1 nM), or MC (Aldrich Chemical Company, Milwaukee, WI) (0.1 nM to 1 µM). Cells were harvested after a treatment period of 24 h, cell extracts were prepared in 1X passive lysis buffer and dual luciferase measurements (Promega Corporation) were performed using a TD-20/20 luminometer (Turner Designs Inc., Sunnyvale, CA). Firefly luciferase activity was normalized to *Renilla* luciferase activity.

To assess the response of mAHR-pGL3 to histone deacetylase inhibitors, cells were transfected with pGL3-Basic (1.5 µg) or mAHR-pGL3 (1.5 µg) using Superfect reagent. After culturing for 24 h, cells were treated with vehicle (0.1% DMSO or ethanol), *n*-butyrate (Aldrich Chemical Company) (0.1 to 5 mM), or trichostatin A (TSA, Sigma Chemical Company) (0.5 to 50 nM). Cells were harvested after a treatment period of 24 h, and firefly luciferase activity was

normalized to cellular protein concentration as determined by the method of Bradford (1976). The effects of *n*-butyrate and TSA on endogenous levels of AHR mRNA and protein were assessed according to the RT-PCR and immunoblot procedures described above.

To assess the response of mAHR-pGL3 to DEX, cells were co-transfected with pGL3-Basic (0.7 µg), pGRE-luc (0.7 µg), or mAHR-pGL3 (0.7 µg) and pRL-TK (0.1 µg) using Superfect reagent. At the same time, cells were also co-transfected with 2.0 µg of a mouse GR expression plasmid, pSVmGR (Dr. John A. Cidlowski, National Institute of Environmental Health Sciences, Research Triangle Park, NC) (Webster et al., 1997), or the empty vector, pSV2 (American Type Culture Collection). After culturing for 24 h, cells were treated with vehicle (0.1% DMSO) or DEX (1 nM to 1 µM). Cells were harvested after a treatment period of 24 h, and firefly luciferase activity was normalized to *Renilla* luciferase activity. Levels of GR protein were assessed according to the immunoblot procedure described above.

Statistical analysis. Data are presented as mean ± SD of the indicated number of determinations. For experiments assessing the effects of DEX on AHR mRNA, protein, TCDD-binding, and DRE-binding, data were analyzed using a repeated-measures design one-way ANOVA followed by a post hoc Newman-Keuls test. For all transfection experiments, data were analyzed initially using a randomized design two-way ANOVA to identify significant influences of the two independent variables in a given experiment (variable 1 = DEX pretreatment or plasmid identity or GR co-transfection; variable 2 = chemical concentration). If a significant effect of variable 1 was identified, a Student's *t* test was performed at each chemical concentration. If a significant effect of variable 2 was identified, a randomized design one-way ANOVA followed by post hoc Newman-Keuls test was performed to identify the chemical

concentrations producing effects that differed from the vehicle control. In all cases, a result was considered to be statistically significant if $p < 0.05$.

Results

Treatment of Hepa-1 cells with DEX, a potent synthetic glucocorticoid, resulted in a 68% increase in the level of AHR mRNA (Fig. 1). Concentrations of DEX (0.1 and 1 μM) that were effective in increasing AHR mRNA levels were also able to activate the GR, as demonstrated by pronounced induction of TAT mRNA (Fig. 1A). The same concentrations of DEX also increased the levels of AHR protein (Fig. 2) and specific [^{3}H]TCDD binding (Fig. 3), and the maximal increases observed in these parameters were 45% and 48%, respectively. A 35% increase in specific [^{3}H]TCDD binding ($p < 0.05$) was also produced following exposure of Hepa-1 cells to 1 and 10 μM concentrations of CORT, the major endogenous rodent glucocorticoid (data not shown). CORT produced similar changes in AHR mRNA and protein levels, but these responses did not achieve statistical significance (data not shown).

The role of the GR in the induction of AHR expression by DEX was tested using the GR antagonist RU486. At a concentration of 1 μM, RU486 blocked the GR-mediated induction of TAT mRNA caused by DEX (0.1 μM) without causing TAT induction on its own (Fig. 4). DEX alone at a concentration of 0.1 μM increased AHR mRNA, protein, and [^{3}H]TCDD binding by 26%, 33%, and 35%, respectively, and these small magnitude increases were not observed when Hepa-1 cells were co-treated with DEX and RU486 (Fig. 4).

To examine whether small changes in AHR protein level caused by DEX resulted in functionally important alterations in the AHR signaling pathway, we first determined the ability of TCCD to transform the cytosolic AHR *in vitro* to a DRE-binding form. By electrophoretic mobility shift assay, the amount of AHR•DRE binding elicited by a maximally effective TCDD concentration did not differ for cytosol isolated from Hepa-1 cells that were previously treated in culture with vehicle or DEX at concentrations of 0.01, 0.1, or 1 μM (Fig. 5).

As a second indicator of AHR function, we examined the ability of TCDD and MC to cause AHR-dependent induction of a luciferase reporter plasmid containing four DREs from the *Cyp1a1* 5'-flank (pGudluc1.1). In the absence of DEX pre-treatment, the maximal induction of pGudluc1.1 luciferase activity by TCDD and MC was 151-fold and 118-fold, respectively (Fig. 6). Following DEX pre-treatment, the maximal induction by TCDD and MC was augmented to 263-fold and 160-fold, respectively (Fig. 6).

To determine if DEX increases the level of AHR mRNA and protein via a transcriptional mechanism, we generated a new luciferase plasmid, mAHR-pGL3, encompassing nucleotides -2451 to +150 of the mouse *Ahr* 5'-flanking region and promoter. The rationale for focusing on this proximal region of the 5'-flank was based on previous reports of an imperfect GRE half-site of uncharacterized function located approximately 1 kb upstream of the major transcription initiation site (Mimura et al., 1994; Fitzgerald et al., 1996; Garrison and Denison, 2000). Before studying the DEX responsiveness of this novel reporter construct, we first confirmed functionality of mAHR-pGL3 by checking for a strong induction in response to histone deacetylase inhibitors, as observed previously with other mouse *Ahr*-based luciferase constructs in Hepa-1 cells (Garrison and Denison, 2000; Garrison et al., 2000). In comparison to the promoterless pGL3-Basic construct, mAHR-pGL3 luciferase activity was increased approximately 7-fold by *n*-butyrate and TSA (Fig. 7A). Consistent with previous studies in wild-type Hepa-1 cells (Zhang et al., 1996; Garrison et al., 2000), the marked effects of histone deacetylase inhibitors on mAHR-pGL3 luciferase activity were accompanied by only small magnitude increases (< 45%) in endogenous AHR mRNA (Fig. 7B) and protein (Fig. 7C) levels. Our initial characterization of the mAHR-pGL3 construct revealed no significant response to the following chemicals in Hepa-1 cells in comparison to the promoterless pGL3-Basic construct (data not shown): TCDD (1 pM to 10 nM), MC (0.1 nM to 1 μM), phenobarbital (10 μM to 1

mM), dehydroepiandrosterone (1 to 100 µM), hydrogen peroxide (0.1 to 1 mM), cumene hydroperoxide (0.1 mM), butylated hydroxytoluene (1 to 100 µM), *trans*-stilbene oxide (1 to 100 µM), progesterone (0.1 to 10 µM), testosterone (0.1 to 100 µM), cyclic AMP (0.01 to 2 mM), retinoic acid (0.1 to 100 nM), phorbol 12-myristate 13-acetate (1 to 500 nM), and 5-aza-2'-deoxycytidine (0.01 to 10 µM).

The final goal of this study was to determine if mAHR-pGL3 luciferase activity is induced by DEX in a GR-dependent manner. Transfection of Hepa-1 cells with a mouse GR expression vector (pSVmGR) elevated cytosolic GR protein levels by approximately 2.4-fold in comparison to cells transfected with the empty vector (pSV2) (Fig. 8A). The promoterless pGL3-Basic construct showed a 12% induction in response to DEX in the absence of exogenous GR, and this induction was augmented to 55% in the presence of exogenous GR (Fig. 8B). The pGRE-luc construct contains consensus GREs from the *TAT* gene and was used as a positive control for GR activation. This reporter plasmid showed a 4.5-fold induction in response to DEX in the absence of exogenous GR, and this induction was augmented to 17.7-fold in the presence of exogenous GR (Fig. 8B). The mAHR-pGL3 construct showed a 29% induction in response to DEX in the absence of exogenous GR, and this induction was augmented to 2.5-fold in the presence of exogenous GR (Fig. 8B).

Discussion

Many factors impact the levels of circulating glucocorticoids, including circadian rhythms, developmental stage, stress, exposure to exogenous steroid therapeutic agents, and diseases of glucocorticoid deficiency and excess. We are interested in the molecular mechanisms by which glucocorticoids modulate the expression of the hepatic AHR and the functional responsiveness to HAHs and PAHs, high priority environmental toxicants.

Glucocorticoids potentiate HAH- and/or PAH-dependent *CYP1A* induction (Nebert and Gelboin, 1969; Sherratt et al., 1989; Celander et al., 1996; Konstandi et al., 2000; Lai et al., 2004). Induction of other AHR target genes is augmented or diminished by glucocorticoids, suggesting multiple molecular mechanisms (Linder et al., 1999). Potentiation of *CYP1A1* induction by glucocorticoids is GR-mediated and involves binding of the GR to multiple GREs initially identified in the first intron of the rat *CYP1A1* gene (Mathis et al., 1989). Conserved GREs are found in the first intron of the *CYP1A1* gene from rat, mouse and human (Linder et al., 1999). However, a dramatic species difference in the *CYP1A1* response exists: DEX potentiates the induction of rat *CYP1A1* by MC at the transcriptional level via a GR•GRE interaction in the first intron, whereas DEX inhibits the induction of human CYP1A1 by MC at the protein level via a GR-independent mechanism (Monostory et al., 2005).

Our study focused on a distinct mechanism that may contribute to potentiated induction of AHR target genes by glucocortiocoids: alteration of AHR expression and function. The first major finding of our study is that DEX increases AHR mRNA, protein and TCDD-binding by approximately 50% in Hepa-1 cells. While the present study was nearing completion, two highly relevant reports appeared in the literature (Dvorak et al., 2007; Sonneveld et al., 2007). Dvorak et al. (2007) found that DEX decreases AHR mRNA levels in HepG2 human hepatoma cells

without affecting AHR protein levels. DEX decreased the induction of an AHR-activated luciferase reporter by TCDD, and TCDD-induced EROD activity was also inhibited. It remains unclear how these effects are produced in the absence of a decrease in AHR protein levels. Sonneveld et al. (2007) found that DEX acts via the GR to augment the induction by TCDD of AHR-activated luciferase reporters, EROD activity, and several endogenous AHR target genes in rodent cells (rat H4IIE and mouse Hepa-1) but not human cells (HepG2 and T47D breast carcinoma cells). DEX increased AHR mRNA levels in rat H4IIE cells, but not in human cells. Together with our current results, these reports solidify the importance of species difference in AHR•GR interactions: glucocorticoids positively impact AHR expression and function in rodent hepatoma cells but negatively impact AHR expression and function in human hepatoma cells.

The magnitude of the increase in AHR levels elicited by DEX in our study was relatively small, in the 50% range. Hepa-1 cells express very high basal levels of AHR protein, with concentrations that are at least an order of magnitude higher than rodent liver levels (Timsit et al., 2002). An upper ceiling may be placed on the glucocorticoid response in Hepa-1 cells by the high basal AHR levels. Also, background levels of cortisol, a lower affinity GR agonist, in the culture medium may have limited the DEX response to a small degree.

The second major finding of our study is that the increase in AHR levels caused by glucocorticoids is mediated by the GR via a transcriptional mechanism. Our evidence for GR involvement in AHR induction by glucocorticoids includes the following: (a) AHR induction occurred at DEX concentrations effective in elevating TAT mRNA, a prototypical GR target; (b) AHR induction by DEX was blocked by RU486, a GR antagonist; (c) induction of the mAHR-pGL3 luciferase reporter by DEX was augmented in the presence of exogenous GR. These findings are consistent with a direct mechanism whereby DEX increases the rate of transcription of the *Ahr* gene via a GR•GRE interaction; however, it is important to consider

other potential indirect mechanisms. We suspect that the pregnane X receptor (PXR) does not play a significant role in the induction of AHR by DEX. While supra-micromolar concentrations of DEX activate murine PXR (Kliewer et al., 1998), we used sub-micromolar concentrations of DEX that selectively activate the GR. RU486 is a murine PXR agonist at high micromolar concentrations (Kliewer et al., 1998), whereas the concentration of RU486 used in the present study (1 μM) was previously shown to have minimal effect on murine PXR activation (Kliewer et al., 1998) and a clear ability to inhibit DEX-induced TAT activity in rat hepatoma cells (Gagne et al., 1985). Sub-micromolar concentrations of DEX act via the GR to stimulate expression of PXR via a transcriptional mechanism (Pascussi et al., 2000). Although PXR may be a potential player in AHR induction by DEX, any role would seem to be minor compared to that for the GR.

We made use of our novel mAHR-pGL3 reporter construct to demonstrate for the first time that DEX increases *Ahr* promoter activity in a GR-dependent manner. The GRE consensus sequence is defined as 5'-GGTACANNNTGTTCT-3' (Lu et al., 2006), with the underlined positions known to tolerate substitution. An imperfect GRE half-site of uncharacterized function (5'-TGATCT-3') located at positions -1009 to -1004 of the mouse *Ahr* gene was noted previously (Mimura et al., 1994; Fitzgerald et al., 1996; Garrison and Denison, 2000). Our bioinformatic analysis identified four potential GREs (with ≤ three mismatches from the consensus) within the cloned region of the mouse *Ahr* 5'-flank contained in the mAHR-pGL3 construct: positions -2432 to -2418; -1073 to -1059; -712 to -698; -237 to -223. The GRE sequence located at positions -2432 to -2418 (5'-GGCACATAGTGTGCT-3') is particularly attractive since the two mismatches from the consensus are located in the underlined positions known to tolerate substitution. We do not yet know if these potential GRE sequences mediate

the induction of the mAHR-pGL3 luciferase activity by DEX in Hepa-1 cells, but these sites are strong candidates for further study.

We and others (Fitzgerald et al., 1996; Garrison and Denison, 2000) found that luciferase reporters driven by the mouse *Ahr* proximal 5'-flank and promoter are refractory to modulation by a wide range of chemicals. Of note, our mAHR-pGL3 construct showed no induction by TCDD or MC although there are putative DREs containing the conserved core (5'-GCGTG-3') at positions +54 to +58, +89 to +93, and +92 to +96. Although the mechanism is uncertain, we confirmed that two histone deacetylase inhibitors caused strong induction of mAHR-pGL3 luciferase activity in Hepa-1 cells (Garrison and Denison, 2000; Garrison et al., 2000).

The third major finding of our study is that a small increase in AHR levels caused by glucocorticoids has a functionally significant impact on aromatic hydrocarbon responsiveness. Pre-treatment of Hepa-1 cells with DEX for 24 h increased AHR levels by approximately 50%, and the subsequent induction of an AHR-activated luciferase reporter (pGudluc1.1) by TCDD and MC was significantly augmented. The pGudluc1.1 reporter construct is devoid of functional GREs and importantly, basal pGudluc1.1 luciferase activity was not elevated in Hepa-1 cells pre-treated for 24 h with DEX relative to vehicle control. Thus, the enhanced responsiveness to TCDD and MC exposure can be attributed to a cellular effect of DEX during the 24 h pre-treatment period and not to any direct effect of DEX on the reporter construct. The increase in AHR levels produced by DEX is a likely mechanistic explanation.

It is puzzling how DEX produces an increase in AHR levels and an enhanced transcriptional response to ligands without an apparent change in AHR•DRE binding. Differences in analytical sensitivity in experimental end-points may be important, but we also note that cells contain distinct pools of AHR proteins that bind ligand but differ in transformation to DNA-binding status (Denison, 1992).

Do changes in AHR levels have a significant impact on the responsiveness of cells to ligands? As addressed in detail in our recent review (Harper et al., 2006), both receptor theory and experimental manipulations demonstrate that changes in AHR levels impact the *CYP1A1* induction response. Our findings support the idea that relatively small increases in AHR protein levels result in significant augmentation of cellular responsiveness to HAHs and PAHs.

In conclusion, glucocorticoids increase AHR levels in mouse hepatoma cells via a GR-dependent transcriptional mechanism. This small increase in AHR levels is associated with an augmented transcriptional response to HAHs and PAHs. This work reveals that glucocorticoid potentiation of *CYP1A1* induction is mediated not only by the presence of GREs in the first intron of the *CYP1A1* gene, but also by increasing AHR expression at the transcriptional level. The present work is important and novel as it provides the first direct evidence for the transcriptional induction of AHR expression by DEX. Alterations in glucocorticoid levels have the potential to modulate the responsiveness of organisms to the toxic and/or adaptive effects of aromatic hydrocarbons. Future studies will address additional details of the molecular mechanisms involved and the *in vivo* relevance of this aspect of cross-talk between the AHR and the GR will be examined in ADX rodent models with glucocorticoid replacement.

Acknowledgments

We thank the following individuals for their kind gifts of plasmids and reagents: Dr. Stephen Safe (Texas A&M University, College Station, TX); Dr. Michael Denison (University of California, Davis, CA); Dr. Gordon Kirby (University of Guelph, Guelph, Ontario, Canada); Dr. John A. Cidlowski (National Institute of Environmental Health Sciences, Research Triangle Park, NC). We thank the following individuals for valuable discussions and assistance: Dr. Patricia Harper, Dr. Allan Okey, Paul Boutros, Rana Sawaya, and Anne Mullen.

References

Abbott BD, Perdew GH, Buckalew AR and Birnbaum LS (1994) Interactive regulation of Ah and glucocorticoid receptors in the synergistic induction of cleft palate by 2,3,7,8-tetrachlorodibenzo-*p*-dioxin and hydrocortisone. *Toxicol Appl Pharmacol* **128:**138-150.

Boutros PC and Okey AB (2004) PUNS: transcriptomic- and genomic-*in silico* PCR for enhanced primer design. *Bioinformatics* **20:**2399-2400.

Bradford MM (1976) A rapid and sensitive method for the quantitation of microgram quantities of protein utilizing the principle of protein-dye binding. *Anal Biochem* **72:**248-254.

Brake PB, Zhang LY and Jefcoate CR (1998) Aryl hydrocarbon receptor regulation of cytochrome P4501B1 in rat mammary fibroblasts: evidence for transcriptional repression by glucocorticoids. *Mol Pharmacol* **54:**825-833.

Carlstedt-Duke JM, Elfstrom G, Hogberg B and Gustafsson J-A (1979) Ontogeny of the rat hepatic receptor for 2,3,7,8-tetrachlorodibenzo-*p*-dioxin and its endocrine independence. *Cancer Res* **39:**4653-4656.

Celander M, Hahn ME and Stegeman JJ (1996) Cytochromes P450 (CYP) in the *Poeciliopsis lucida* hepatocellular carcinoma cell line (PLHC-1): dose- and time-dependent glucocorticoid potentiation of CYP1A induction without induction of CYP3A. *Arch Biochem Biophys* **329:**113-122.

Chomczynski P and Sacchi N (1987) Single-step method of RNA isolation by acid guanidinium thiocyanate-phenol-chloroform extraction. *Anal Biochem* **162:**156-159.

Cuthill S, Poellinger L and Gustafsson J-A (1987) The receptor for 2,3,7,8-tetrachlorodibenzo-*p*-dioxin in the mouse hepatoma cell line Hepa-1c1c7: a comparison with the glucocorticoid receptor and the mouse and rat hepatic dioxin receptors. *J Biol Chem* **262:**3477-3481.

Denison MS (1992) Heterogeneity of rat hepatic Ah-receptor: identification of two receptor forms which differ in their biochemical properties. *J Biochem Toxicol* **7:**249-256.

Dvorak Z, Vrzal R, Pavek P and Ulrichova J (2007) An evidence for regulatory cross-talk between aryl hydrocarbon receptor and glucocorticoid receptor in HepG2 cells. *Physiol Res*., in press. [e-pub ahead of print, 30 May 2007]

Fitzgerald CT, Fernandez-Salguero P, Gonzalez FJ, Nebert DW and Puga A (1996) Differential regulation of mouse Ah receptor gene expression in cell lines of different tissue origins. *Arch Biochem Biophys* **333:**170-178.

Gagne D, Pons M and Philibert D (1985) RU 38486: a potent antiglucocorticoid *in vitro* and *in vivo*. *J Steroid Biochem* **23:**247-251.

Garrison PM and Denison MS (2000) Analysis of the murine AhR gene promoter. *J Biochem Mol Toxicol* **14:**1-10.

Garrison PM, Rogers JM, Brackney WR and Denison MS (2000) Effects of histone deacetylase inhibitors on the Ah receptor gene promoter. *Arch Biochem Biophys* **374:**161-171.

Garrison PM, Tullis K, Aarts JMMJG, Brouwer A, Giesy JP and Denison MS (1996) Species-specific recombinant cell lines as bioassay systems for the detection of 2,3,7,8-tetrachlorodibenzo-*p*-dioxin-like chemicals. *Fund Appl Toxicol* **30:**194-203.

Gerbal-Chaloin S, Daujat M, Pascussi JM, Pichard-Garcia L, Vilarem MJ and Maurel P (2002) Transcriptional regulation of *CYP2C9* gene: role of glucocorticoid receptor and constitutive androstane receptor. *J Biol Chem* **277:**209-217.

Giannone JV, Li W, Probst M and Okey AB (1998) Prolonged depletion of AH receptor without alteration of receptor mRNA levels after treatment of cells in culture with 2,3,7,8-tetrachlorodibenzo-*p*-dioxin. *Biochem Pharmacol* **55:**489-497.

Gorski JR, Rozman T, Greim H and Rozman K (1988) Corticosterone modulates acute toxicity of 2,3,7,8-tetrachlorodibenzo-*p*-dioxin (TCDD) in male Sprague-Dawley rats. *Fund Appl Toxicol* **11:**494-502.

Harper PA, Riddick DS and Okey AB (2006) Regulating the regulator: factors that control levels and activity of the aryl hydrocarbon receptor. *Biochem Pharmacol* **72:**267-279.

Kliewer SA, Moore JT, Wade L, Staudinger JL, Watson MA, Jones SA, McKee DD, Oliver BB, Willson TM, Zetterstrom RH, Perlmann T and Lehmann JM (1998) An orphan nuclear receptor activated by pregnanes defines a novel steroid signaling pathway. *Cell* **92:**73-82.

Konstandi M, Johnson E, Lang MA, Camus-Radon AM and Marselos M (2000) Stress modulates the enzymatic inducibility by benzo[*a*]pyrene in the rat liver. *Pharmacol Res* **42:**205-211.

Lai KP, Wong MH and Wong CKC (2004) Modulation of AhR-mediated CYP1A1 mRNA and EROD activities by 17ß-estradiol and dexamethasone in TCDD-induced H4IIE cells. *Toxicol Sci* **78:**41-49.

Linder MW, Falkner KC, Srinivasan G, Hines RN and Prough RA (1999) Role of canonical glucocorticoid responsive elements in modulating expression of genes regulated by the aryl hydrocarbon receptor. *Drug Metab Rev* **31:**247-271.

Lu NZ, Wardell SE, Burnstein KL, Defranco D, Fuller PJ, Giguere V, Hochberg RB, McKay L, Renoir JM, Weigel NL, Wilson EM, McDonnell DP and Cidlowski JA (2006) International Union of Pharmacology. LXV. The pharmacology and classification of the nuclear receptor superfamily: glucocorticoid, mineralocorticoid, progesterone, and androgen receptors. *Pharmacol Rev* **58:**782-797.

Mathis JM, Houser WH, Bresnick E, Cidlowski JA, Hines RN, Prough RA and Simpson ER (1989) Glucocorticoid regulation of the rat cytochrome P450c (P450IA1) gene: receptor binding within intron I. *Arch Biochem Biophys* **269:**93-105.

Mimura J, Ema M, Sogawa K, Ikawa S and Fujii-Kuriyama Y (1994) A complete structure of the mouse Ah receptor gene. *Pharmacogenetics* **4:**349-354.

Monostory K, Kohalmy K, Prough RA, Kobori L and Vereczkey L (2005) The effect of synthetic glucocorticoid, dexamethasone on CYP1A1 inducibility in adult rat and human hepatocytes. *FEBS Lett* **579:**229-235.

Nebert DW and Gelboin HV (1969) The *in vivo* and *in vitro* induction of aryl hydrocarbon hydroxylase in mammalian cells of different species, tissues, strains and developmental and hormonal states. *Arch Biochem Biophys* **134:**76-89.

Pascussi JM, Drocourt L, Fabre JM, Maurel P and Vilarem MJ (2000) Dexamethasone induces pregnane X receptor and retinoid X receptor-α expression in human hepatocytes: synergistic increase of *CYP3A4* induction by pregnane X receptor activators. *Mol Pharmacol* **58:**361-372.

Pollenz RS, Sattler CA and Poland A (1994) The aryl hydrocarbon receptor and aryl hydrocarbon receptor nuclear translocator protein show distinct subcellular localizations in Hepa 1c1c7 cells by immunofluorescence microscopy. *Mol Pharmacol* **45:**428-438.

Prokipcak RD and Okey AB (1988) Physicochemical characterization of the nuclear form of *Ah* receptor from mouse hepatoma cells exposed in culture to 2,3,7,8-tetrachlorodibenzo-*p*-dioxin. *Arch Biochem Biophys* **267:**811-828.

Riddick DS, Huang Y, Harper PA and Okey AB (1994) 2,3,7,8-Tetrachlorodibenzo-*p*-dioxin versus 3-methylcholanthrene: comparative studies of Ah receptor binding, transformation, and induction of *CYP1A1*. *J Biol Chem* **269:**12118-12128.

Safe SH (1995) Modulation of gene expression and endocrine response pathways by 2,3,7,8-tetrachlorodibenzo-*p*-dioxin and related compounds. *Pharmacol Ther* **67:**247-281.

Sakuma T, Kitajima K, Nishiyama M, Endo Y, Miyauchi K, Jarukamjorn K and Nemoto N (2004) Collaborated regulation of female-specific murine *Cyp3a41* gene expression by growth and glucocorticoid hormones. *Biochem Biophys Res Commun* **314:**495-500.

Sherratt AJ, Banet DE, Linder MW and Prough RA (1989) Potentiation of 3-methylcholanthrene induction of rat hepatic cytochrome P450IA1 by dexamethesone *in vivo*. *J Pharmacol Exp Ther* **249:**667-672.

Sonneveld E, Jonas A, Meijer OC, Brouwer A and van der Burg B (2007) Glucocorticoid-enhanced expression of dioxin target genes through regulation of the rat aryl hydrocarbon receptor. *Toxicol Sci* **99:**455-469.

Timsit YE, Chia FS-C, Bhathena A and Riddick DS (2002) Aromatic hydrocarbon receptor expression and function in liver of hypophysectomized male rats. *Toxicol Appl Pharmacol* **185:**136-145.

Webster JC, Jewell CM, Bodwell JE, Munck A, Sar M and Cidlowski JA (1997) Mouse glucocorticoid receptor phosphorylation status influences multiple functions of the receptor protein. *J Biol Chem* **272:**9287-9293.

Wiebel FJ and Cikryt P (1990) Dexamethasone-mediated potentiation of P450IA1 induction in H4IIEC3/T hepatoma cells is dependent on a time-consuming process and associated with induction of the Ah receptor. *Chemico-Biol Interact* **76:**307-320.

Zhang JZ, Watson AJ, Probst MR, Minehart E and Hankinson O (1996) Basis for the loss of aryl hydrocarbon receptor gene expression in clones of a mouse hepatoma cell line. *Mol Pharmacol* **50:**1454-1462.

Footnotes

Supported by the Canadian Institutes of Health Research Grant MOP-42399 (D.S.R.).

K.A.B. was the recipient of a Postgraduate Scholarship from the Natural Sciences and Engineering Research Council of Canada.

Address correspondence to: David S. Riddick, Department of Pharmacology & Toxicology, Medical Sciences Building, University of Toronto, Toronto, Ontario, Canada, M5S 1A8.

E-mail: david.riddick@utoronto.ca

Figure Legends

FIG. 1. Effect of DEX treatment on AHR mRNA levels in Hepa-1 cells. (A) Vistra Green-stained polyacrylamide gel depicting relative AHR and ß-actin mRNA levels is shown in the upper panel and the corresponding image in the lower panel shows the relative level of TAT mRNA for each sample, included as a positive control for GR activation. Representative results are shown for a single RNA isolation out of three independent experiments conducted. (B) Semiquantitative image analysis of AHR mRNA levels. RT-PCR data are expressed as a percentage of the mean of the vehicle control and represent the mean ± SD of determinations from three independent RNA isolations. AHR signal intensity was normalized to that of ß-actin for each sample. *, significantly different ($p < 0.05$) from vehicle control; **, significantly different ($p < 0.01$) from vehicle control, based on a repeated-measures design one-way ANOVA followed by a post hoc Newman-Keuls test.

FIG. 2. Effect of DEX treatment on cytosolic AHR protein levels in Hepa-1 cells. (A) Immunoblot analysis of cytosolic protein (10 µg) using polyclonal antibody directed against mouse AHR. Representative results are shown for a single cytosol isolation out of three independent experiments conducted. (B) Semiquantitative image analysis of AHR protein levels. Immunoblot data are expressed as a percentage of the mean of the vehicle control and represent the mean ± SD of determinations from three independent cytosol isolations. *, significantly different ($p < 0.05$) from vehicle control, based on a repeated-measures design one-way ANOVA followed by a post hoc Newman-Keuls test.

FIG. 3. Effect of DEX treatment on [^{3}H]TCDD binding to cytosolic AHR in Hepa-1 cells. (A) Sucrose density gradient profiles for each DEX treatment group, with specific [^{3}H]TCDD binding to the AHR localized to the ~9S region of the gradients (fractions 8 to 17). Representative results are shown for a single cytosol isolation out of three independent experiments conducted. (B) Quantitative analysis of specific [^{3}H]TCDD binding to the ~9S cytosolic AHR. Data are expressed as a percentage of the mean of the vehicle control and represent the mean ± SD of determinations from three independent cytosol isolations. Cytosol from the vehicle treatment group had a mean concentration of 1438 fmol AHR/mg cytosolic protein. *, significantly different ($p < 0.05$) from vehicle control; **, significantly different ($p < 0.01$) from vehicle control, based on a repeated-measures design one-way ANOVA followed by a post hoc Newman-Keuls test.

FIG. 4. Effect of RU486 on induction of AHR mRNA, protein and [^{3}H]TCDD binding levels by DEX in Hepa-1 cells. The upper panel shows a Vistra Green-stained polyacrylamide gel depicting the relative level of TAT mRNA for each sample, included as a positive control for GR activation. Representative results are shown for a single RNA isolation out of three independent experiments conducted. The lower panel shows the quantitative analysis of AHR mRNA, protein and [^{3}H]TCDD binding levels. Data are expressed as a percentage of the mean of the vehicle control and represent the mean ± SD of determinations from three independent RNA and cytosol isolations. For RT-PCR analysis, AHR signal intensity was normalized to that of ß-actin for each sample. Cytosol from the vehicle treatment group had a mean concentration of 1359 fmol AHR/mg cytosolic protein. *, significantly different ($p < 0.05$) from vehicle control; †, significantly different ($p < 0.05$) from all other treatment groups; ††, significantly different

($p < 0.01$) from all other treatment groups, based on a repeated-measures design one-way ANOVA followed by a post hoc Newman-Keuls test.

FIG. 5. Effect of DEX treatment in Hepa-1 cells on the ability of TCDD to transform the cytosolic AHR into its DRE-binding form. (A) Electrophoretic mobility shift assay showing the TCDD-inducible interaction of transformed cytosolic AHR with a ^{32}P-labeled double-stranded oligonucleotide containing a DRE sequence (indicated by arrow). F indicates the free DRE probe. Representative results are shown for a single cytosol isolation out of three independent experiments conducted. (B) Semiquantitative image analysis of TCDD-inducible DRE binding. Data are expressed as a percentage of the mean of the vehicle control and represent the mean ± SD of determinations from three independent cytosol isolations. No statistically significant differences among treatment groups, based on a repeated-measures design one-way ANOVA. Note that the image is taken from an extended autoradiographic film exposure, whereas the quantitative analysis was performed at earlier exposure times when signals were within the Phosphorimager dynamic range.

FIG. 6. Effect of DEX pretreatment on the concentration-dependent induction of pGudluc1.1 luciferase activity by TCDD and MC in transiently transfected Hepa-1 cells. (A) Concentration-dependent induction of pGudluc1.1 luciferase activity by TCCD following treatment in the absence or presence of DEX. (B) Concentration-dependent induction of pGudluc1.1 luciferase activity by MC following treatment in the absence or presence of DEX. Firefly luciferase activity was normalized to *Renilla* luciferase activity. Data are expressed as fold increase over vehicle control and represent the mean ± SD of three determinations. Data were analyzed initially using a randomized design two-way ANOVA to identify significant DEX pretreatment

and chemical concentration effects. ***, significantly different ($p < 0.001$) from vehicle control, based on a randomized design one-way ANOVA followed by a post hoc Newman-Keuls test. †, significantly different ($p < 0.05$) from no DEX treatment; ††, significantly different ($p < 0.01$) from no DEX treatment; †††, significantly different ($p < 0.001$) from no DEX treatment, based on Student's *t* test.

FIG. 7. Concentration-dependent effects of the histone deacetylase inhibitors, *n*-butyrate and TSA, on mAHR-pGL3 luciferase activity in transiently transfected Hepa-1 cells and on endogenous AHR mRNA and protein levels. (A) Luciferase activity analysis. Firefly luciferase activity was normalized to cellular protein concentration. Data are expressed as fold increase over vehicle control and represent the mean ± SD of three determinations. Data were analyzed initially using a randomized design two-way ANOVA to identify significant plasmid identity and chemical concentration effects. *, significantly different ($p < 0.05$) from vehicle control; **, significantly different ($p < 0.01$) from vehicle control; ***, significantly different ($p < 0.001$) from vehicle control, based on a randomized design one-way ANOVA followed by a post hoc Newman-Keuls test. †, significantly different ($p < 0.05$) from pGL3-Basic; ††, significantly different ($p < 0.01$) from pGL3-Basic; †††, significantly different ($p < 0.001$) from pGL3-Basic, based on Student's *t* test. (B) RT-PCR analysis of AHR and ß-actin mRNA levels following treatment of cells with *n*-butyrate (left panel) or TSA (right panel) for 24 h. Representative results are shown for a single RNA isolation out of two independent experiments conducted. (C) Immunoblot analysis of AHR protein levels following treatment of cells with *n*-butyrate (left panel) or TSA (right panel) for 24 h. Representative results are shown for a single cytosol isolation out of two independent experiments conducted.

FIG. 8. Concentration-dependent effects of DEX on mAHR-pGL3 luciferase activity in transiently transfected Hepa-1 cells in the absence and presence of exogenous GR.
(A) Immunoblot analysis of GR protein levels. Cells were transfected with a mouse GR expression plasmid (pSVmGR) or the empty vector (pSV2) or left untransfected (-). Cytosol was harvested 48 h after transfection. Representative results are shown for a single cytosol isolation out of two independent experiments conducted. (B) Luciferase activity analysis. Firefly luciferase activity was normalized to *Renilla* luciferase activity. Data are expressed as fold increase over vehicle control and represent the mean ± SD of three determinations. Data were analyzed initially using a randomized design two-way ANOVA to identify significant GR co-transfection and chemical concentration effects. *, significantly different ($p < 0.05$) from vehicle control; **, significantly different ($p < 0.01$) from vehicle control; ***, significantly different ($p < 0.001$) from vehicle control, based on a randomized design one-way ANOVA followed by a post hoc Newman-Keuls test. †, significantly different ($p < 0.05$) from pSV2; †††, significantly different ($p < 0.001$) from pSV2, based on Student's *t* test.

Figure 1

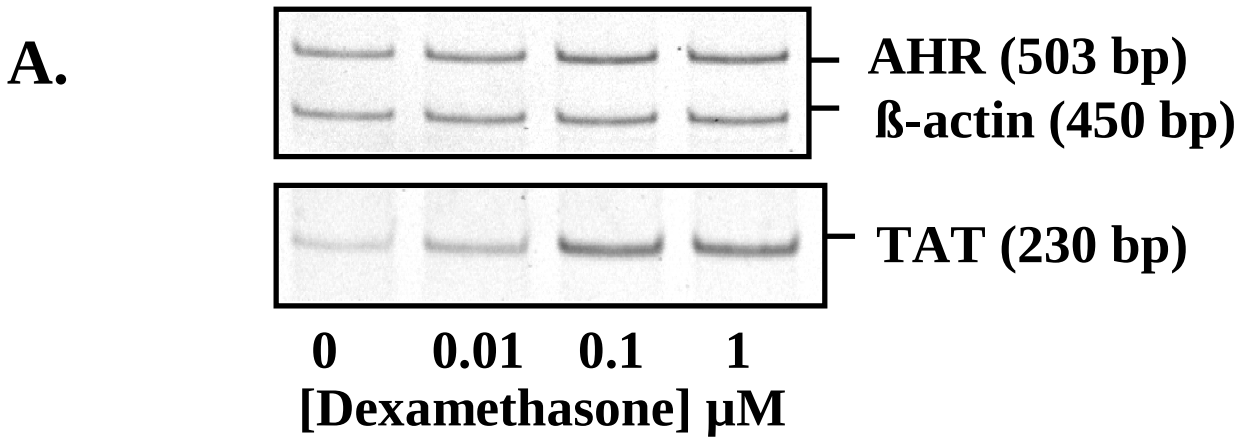

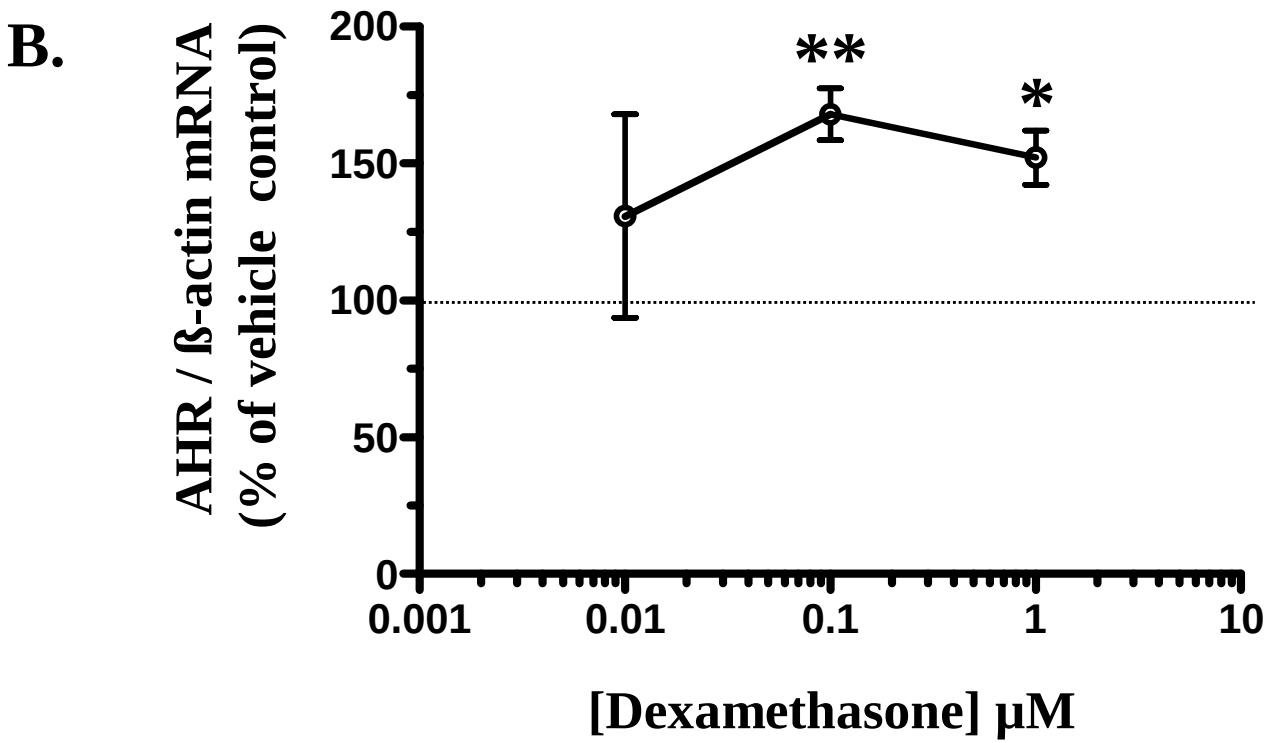

Figure 2

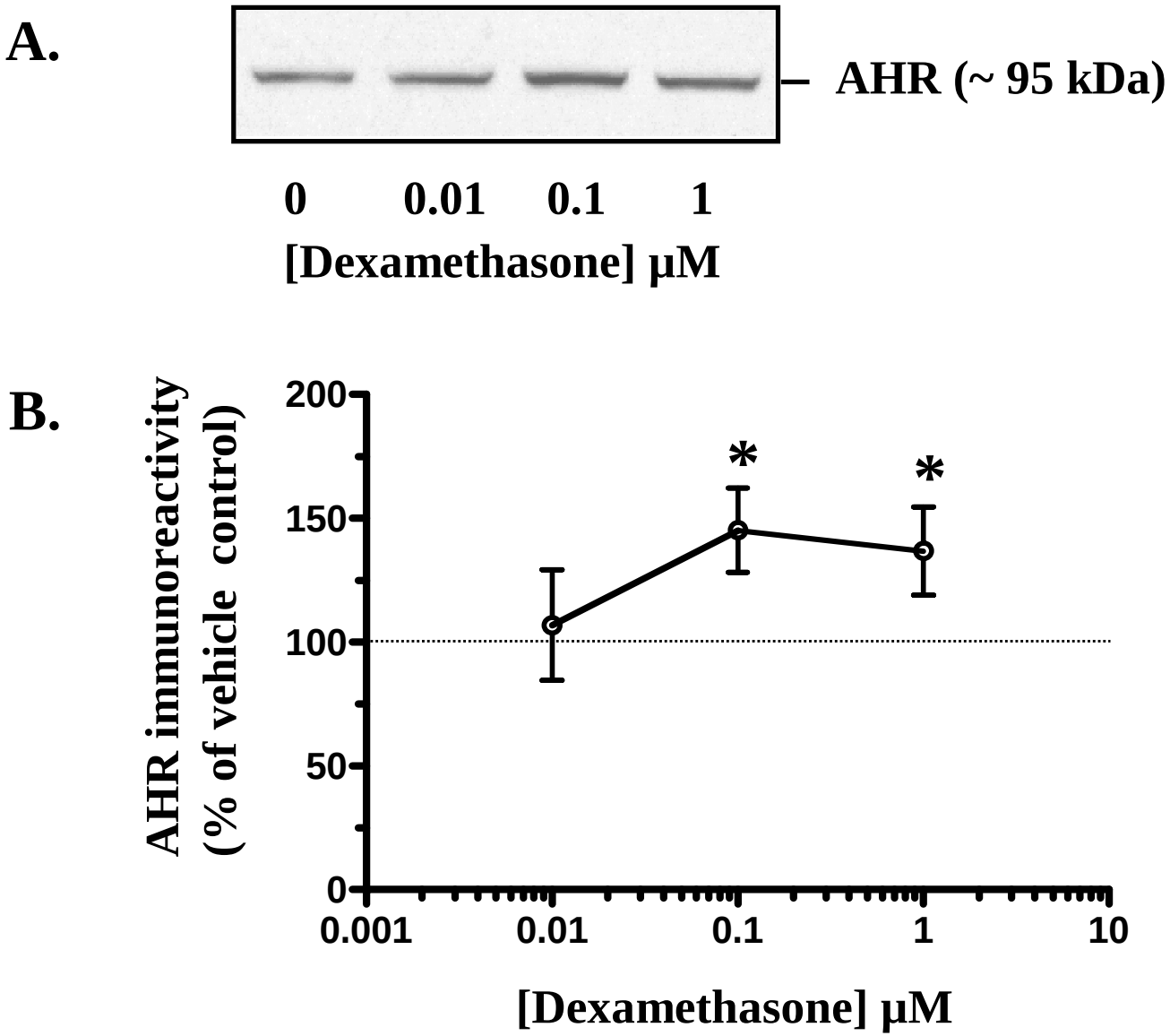

Figure 3

A.

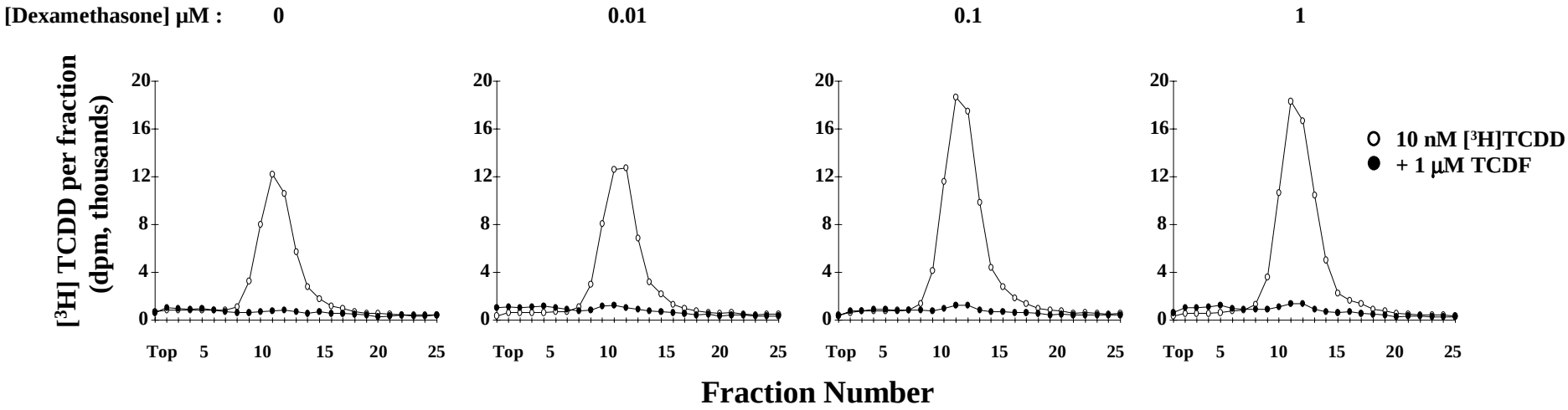

B.

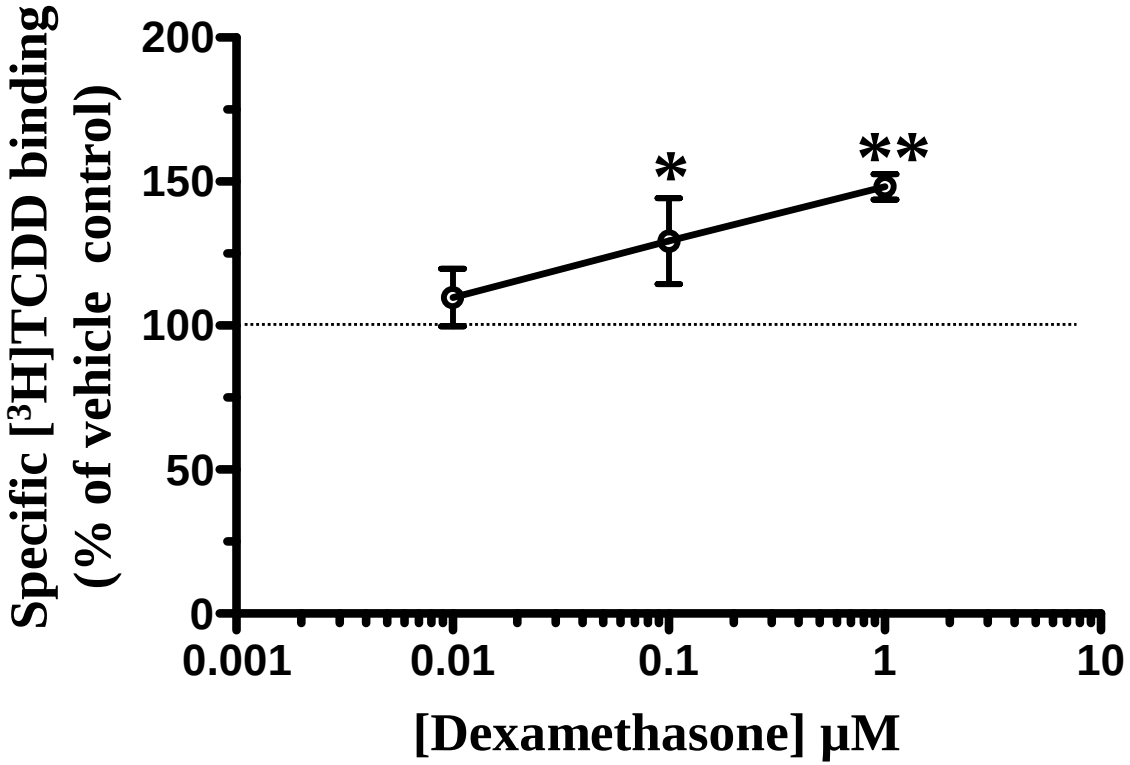

Figure 4

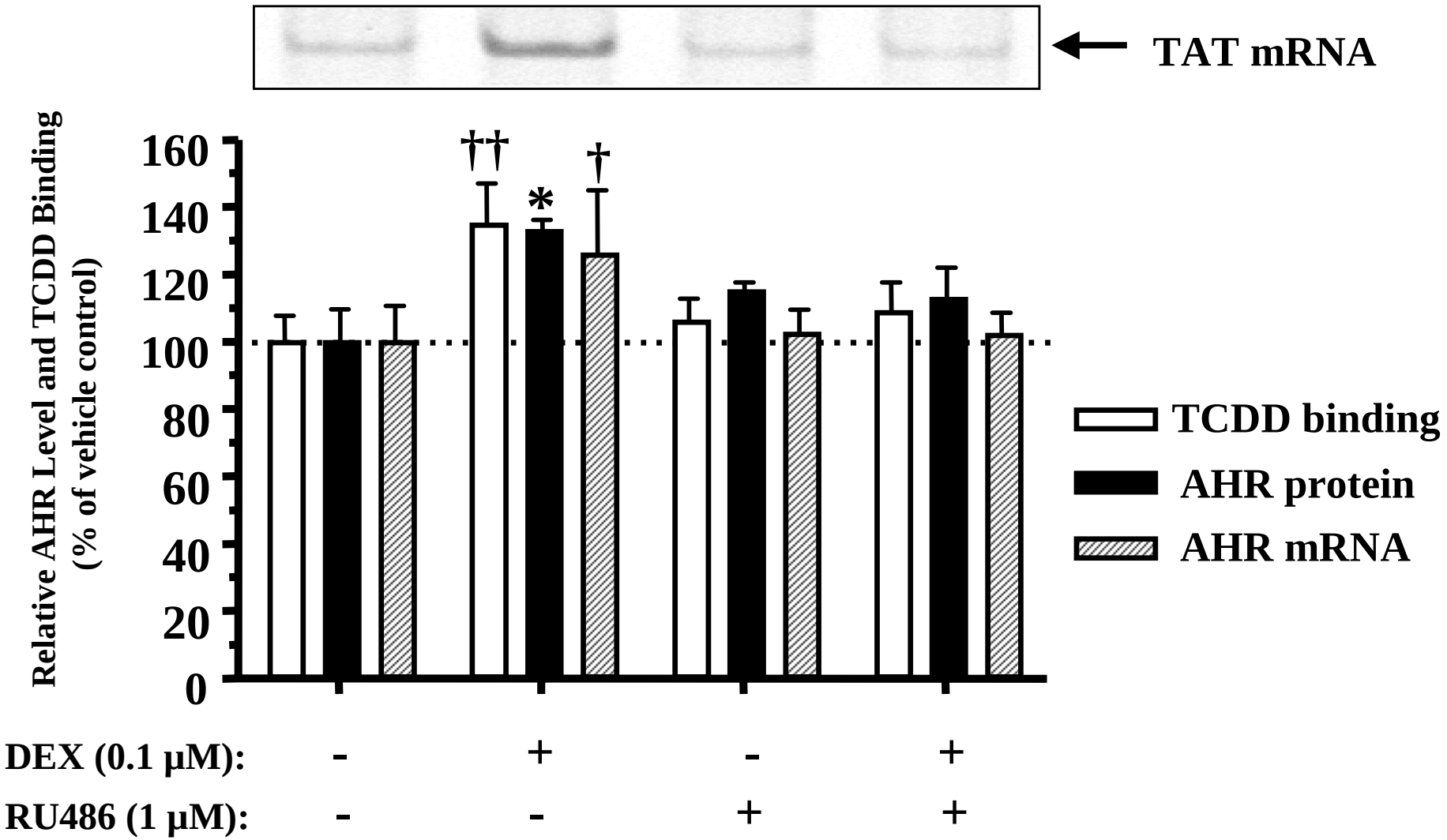

Figure 5

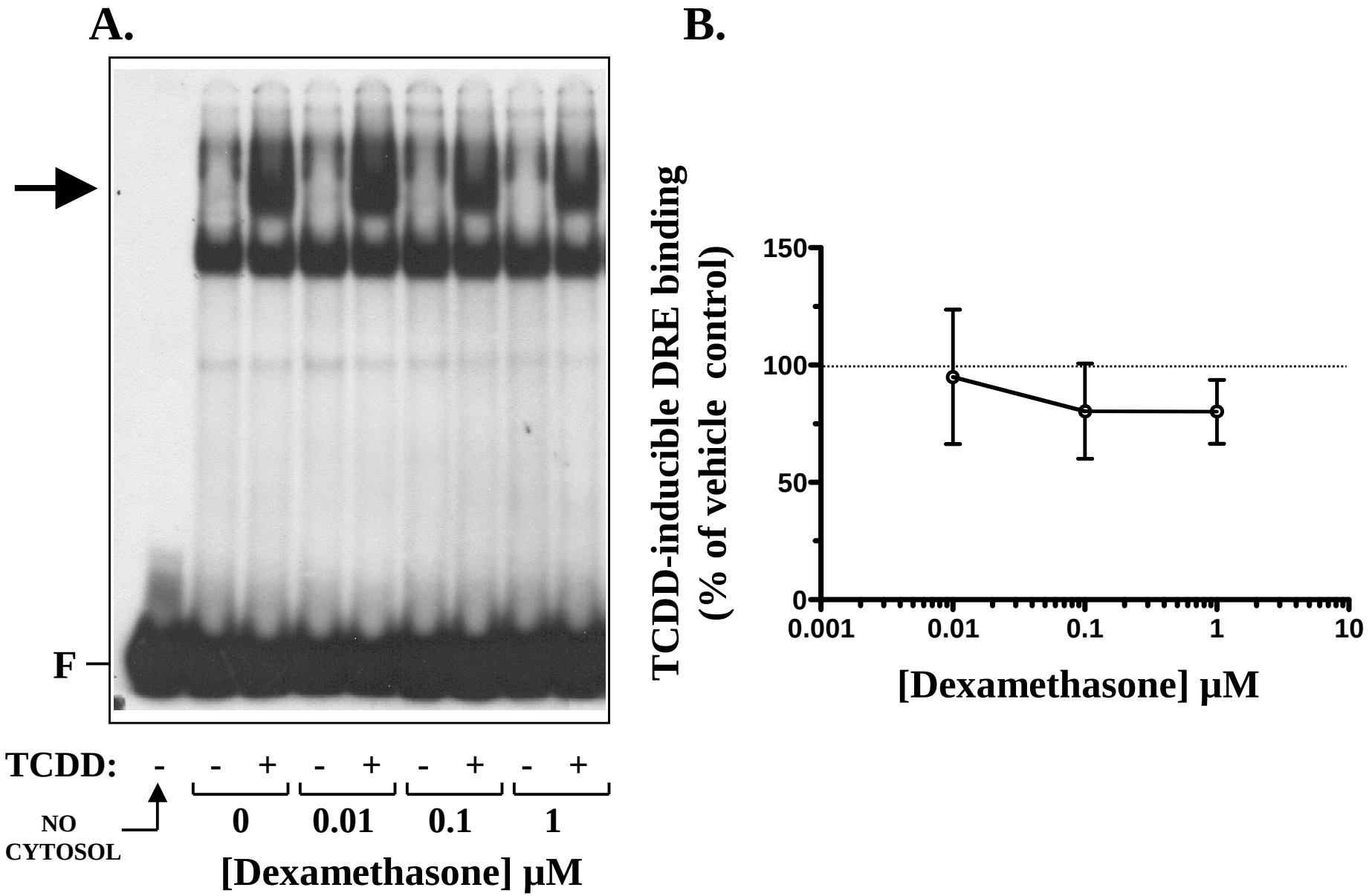

Figure 6

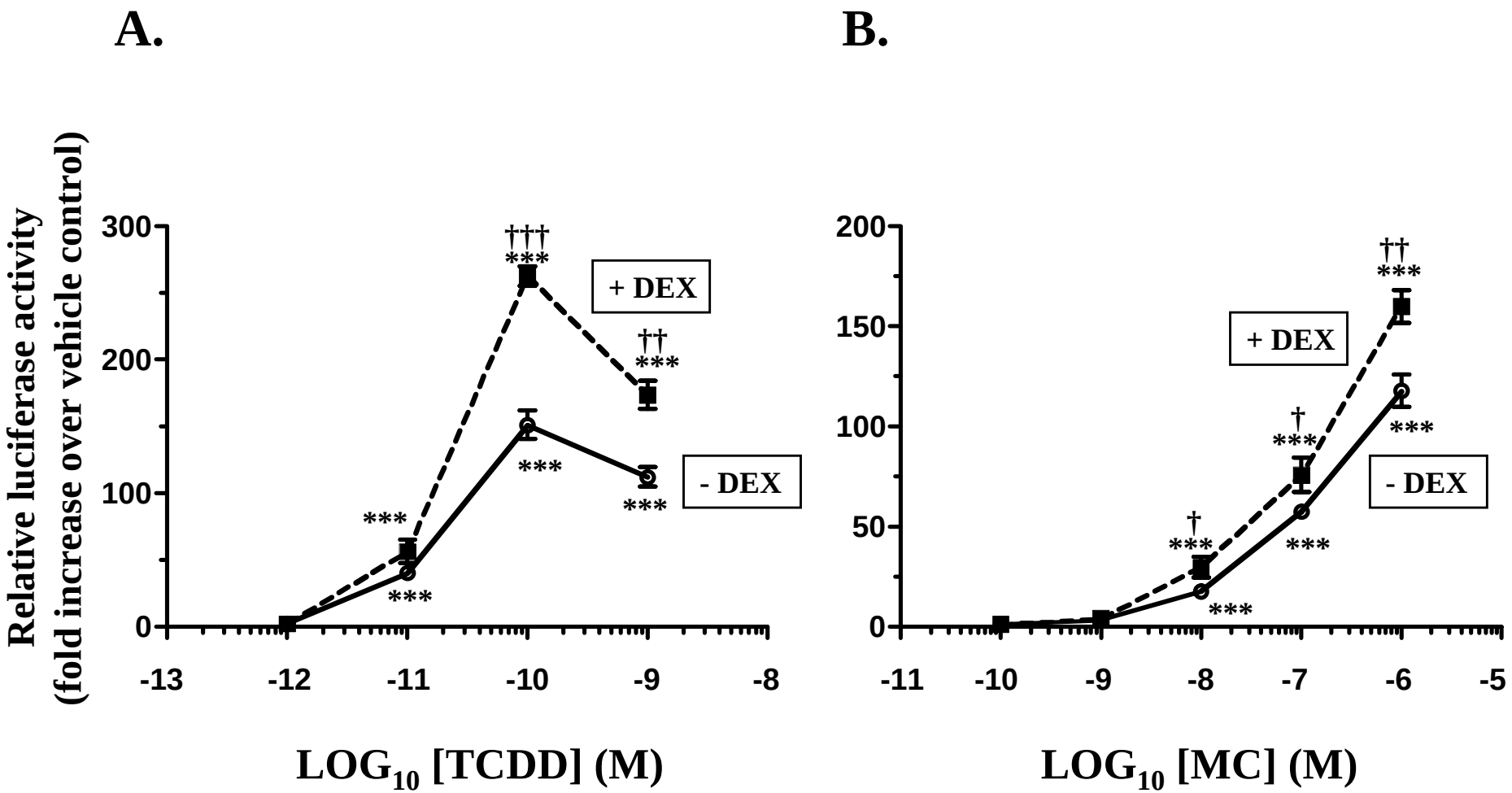

Figure 7

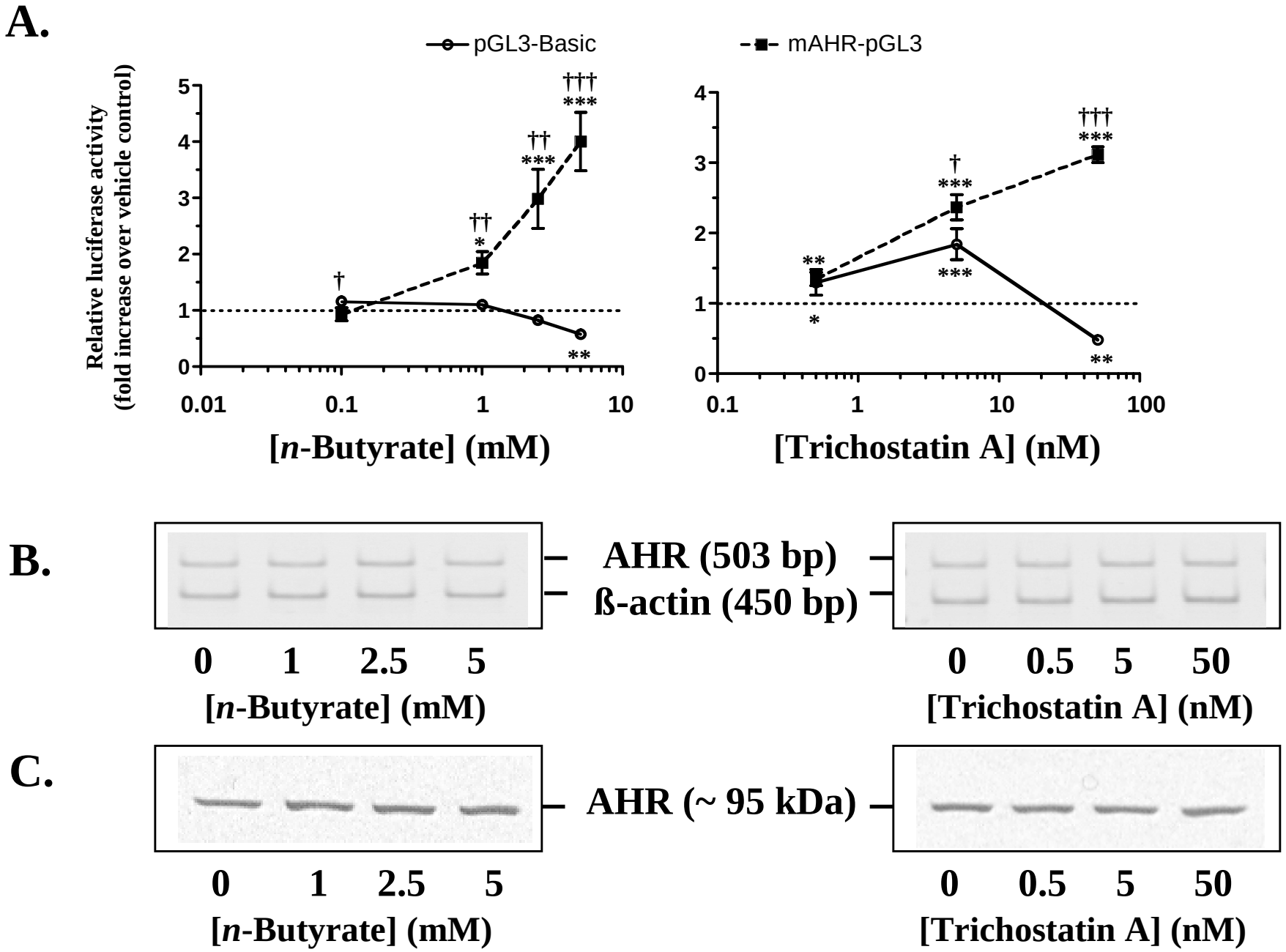

Figure 8